



Sudan University of Science and Technology
College of Petroleum Engineering and Technology
Department of petroleum Engineering



Determining mud weight window to overcome wellbore instability with case study Fula North Field in Sudan

**تحديد نافذة وزن سائل الحفر للتغلب على عدم إستقرارية البئر
مع دراسة حالة: حقل الفولة الشمالي-السودان**

**Project submitted to Collage of petroleum Engineering & Technology for
partial fulfilment of the requirement for B.sc Degree**

by:

- Basheer Rafiq Saif Al-Sharjabi
- Hassan Emad-Aldeen Hassan
- Khalid Omer Ibrahim
- Marwa Ahmed

Supervised by:

- Dr. Yousif Altaher Bagadi

October - 2018

Determining mud weight window to overcome wellbore instability with case study Fula North Field in Sudan

Graduation project submitted to college of Petroleum Engineering and Technology in Sudan University of Science and Technology

Submitted in Partial Fulfillment of the Requirement for the Bachelor of Engineering (Hones) Degree in Transportation and Refining Engineering

Prepared by:

- Basheer Rafiq Saif
- Hassan Emad Aldeen Hassan
- Khalid Omer Ibrahim
- Marwa Ahmed

Supervised by:

- Dr. Yousif Altaher Bagadi

This project is approved by College of Petroleum Engineering and Technology to petroleum Department

- Supervisor: Dr. Yousif Altaher Bagadi

Signature:

Head of Department: Dr. Abd-Alwhab Mohammed Fadul

Signature:

Dean of College: Dr. Tagwa Ahmed Musa

Signature:.....

Date: 21 /10/2018

الإستهلال

قال تعالى:

{ وَمَا تَوْفِيقِي إِلَّا بِاللَّهِ عَلَيْهِ تَوَكَّلْتُ وَإِلَيْهِ أُنِيبُ }

سورة هود الآية (88)

Dedication

We dedicate this project to our parents for the love and support they have provided throughout our entire life, they have been there for every decision we have made and help our dreams become reality, to our friends and families for their help and encouragement.

ACKNOWLEDGEMENT

Acknowledgment First of all, we would like to thank Great and Almighty God who gave us the power to fulfill this study. Thanks, should be given to our supervisor's We would like to express our appreciation to our supervisor: **Dr. Yusef Altaher**

Baghadi

Furthermore, we thank the staff and lecturers at the university and our friends of various backgrounds that always supported us. Our special thanks also due to **Mr.Ateeg Abd-erazig Mohammed** for providing continuous assistance.

Thanks and apologies to others whose contributions we may have missed or forgotten to acknowledge.

Last, but certainly not least, our heartfelt gratitude goes to our families for their patience, loving support and continual encouragement for their continuous advice and encouragement throughout the entire course of our study.

The greatest thanks for all which help us until this research completed and reached to this feature at top of them.

ABSTRACT

Wellbore stability-related problems are one of the main sources of time and money losses in any drilling operation. This is the reason why, in the last years, many improvements have been made in this specific field of research. The improvements are based on a better knowledge of the mechanisms that originate rock failure. One of the key parameters to be controlled and monitored while drilling is that of the mud weight. In order to avoid well instability, a graphical representation of the safe mud weight window is presented. This graphical solution is intended to ease the estimation of the values that guarantee well stability, either in tension or compression, at any depth, based on the geomechanical properties of the formations crossed while drilling.

During drilling operations for the Baleela oil field in the Abu Gabera formation in Sudan, loss circulation has been identified as a geomechanical problem for several wells. In this project a one-dimension geological earth model of the Abu Gabera formation is compiled based on its state of stress and rock strength parameters.

The mechanical earth model depends on the principle in-situ stresses which obtained from wireline logging. Rock strength properties obtained from empirical equations. Therefore, we can minimize non-productive time NPT and the cost of drilling significantly by precluding some drilling problems. Based on the MEM results, the mud pressure window is calculated and a mud weight is recommended for the Abu Gabera formation. The field case provides proof that the Matlab software is a very good tool for predicting a safe mud weight window.

التجريد

تعد المشاكل المتعلقة باستقرار حفرة البئر واحدة من المصادر الرئيسية لخسائر الوقت والمال في أي عملية حفر. هذا هو السبب في أنه، في السنوات الأخيرة، تم إجراء العديد من التحسينات في هذا المجال البحثي المحدد. تستند التحسينات إلى معرفة أفضل بالآليات التي تنشأ من فشل الصخور. واحدة من المعلومات الرئيسية التي يتعين التحكم فيها ومراقبتها أثناء الحفر هي وزن الطين (سائل الحفر). من أجل تجنب عدم الاستقرار بشكل جيد، يتم تقديم تمثيل بياني لنافذة وزن الطين الآمنة. يهدف هذا الحل البياني إلى التخفيف من تقدير القيم التي تضمن ثبات البئر، سواء في الشد أو الضغط، في أي عمق، بناءً على الخصائص الجيوميكانيكية للتراكيب التي تم تقاطعه أثناء الحفر.

خلال عمليات الحفر في حقل بليلة (حقل الفولا الشمالي) النفطي في تكوين أبو جابرة في السودان، تم تحديد فقدان سائل الحفر كمسكلة جيوميكانية لعدة آبار. في هذا المشروع تم تكوين نموذج جيوميكانيكي أحادي البعد لتكوين أبو جابرة استناداً إلى حالة الإجهاد ومعلومات قوة الصخور.

يعتمد النموذج الأرضي الجيوميكانيكي على الإجهادات الأساسية في الموقع والتي تم الحصول عليها من تسجيلات الآبار. وأيضاً خصائص قوة الصخور التي تم الحصول عليها من المعادلات التجريبية. لذلك، يمكننا تقليل الوقت غير الإنتاجي وتكلفة الحفر بشكل كبير عن طريق منع بعض مشاكل الحفر. استناداً إلى النتائج، يتم حساب نافذة ضغط الطين ويوصى بوزن الطين الملائم لتكوين أبو جابرة. حالة الحقل المدروسة دليلاً على أن برنامج الماتلاب هو أداة جيدة جداً للتنبؤ بإطار وزن الطين الآمن.

Table of content

الإستهلال	iii
Dedication	iv
Acknowledgement	v
Abstract	vi
التجريد.....	vii
Table of content	viii
List of Figures	xi
List of tables.....	xiii
Chapter 1	- 1 -
Introduction.....	- 1 -
1.1. Introduction.....	- 1 -
1.2. Objectives:	- 4 -
1.3. Problem statement:.....	- 5 -
Chapter two	- 6 -
Literature review	- 6 -
Chapter three	- 9 -
Methodology	- 9 -
3.1. Introduction.....	- 9 -

3.2. Matlab Program (GUI).....	- 10 -
3.2.1 The GUI contains	- 10 -
3.3. Overburden Stress	- 11 -
3.4. Rock Strength Parameters.....	- 13 -
3.5. Pore Pressure.....	- 14 -
3.7.1. Eaton’s Method.....	- 16 -
3.7.2. Bowers’ Method.....	- 16 -
3.6. Minimum Horizontal Stress.....	- 17 -
3.7. Maximum horizontal stress.....	- 18 -
3.8. Internal Friction Angle.....	- 20 -
3.9. Fracture gradient	- 20 -
3.10. Mohr-coulomb failure criterion	- 21 -
3.11. Estimating Tensile strength	- 21 -
Chapter four	- 22 -
Results and discussion	- 22 -
4.1. The quantification of wellbore instability:	- 22 -
4.1.1. Determining magnitude and direction of in-situ earth stresses	- 22 -
-	
4.1.2. Determination of rock properties:.....	- 23 -
4.1.3. Rock failure:.....	- 24 -
4.2. Procedures for determining safe mud weights to prevent hole collapse: - 26 -	

4.3. Calculations.....	- 27 -
4.3.1. Poisson Ratio, Shear and young's Modulus Calculations	- 28 -
4.3.2. Overburden pressure:	- 29 -
4.4. Result:	- 34 -
Chapter five	- 41 -
Conclusion and recommendation.....	- 41 -
references	- 42 -

List of Figures

(Fig. 1.1) Typical borehole problems.(Mitchell, Miska, Aadnøy, & Engineers, 2011)	- 3 -
Figure (3.1) Depicted MEM Flowchart	- 9 -
Figure (3.2) Work flow of pore pressure estimation from MSE and DE ('DESME') method.(Zoback, 2007)	- 16 -
Figure (4-1) Triaxial Rock Testing.(H.Rabia, 2002)	- 24 -
Figure (4-2) Mohr Envelop. (H.Rabia, 2002)	- 25 -
Figure (4-3) Failure stresses using the triaxial test results and Mohr-Coulomb model.(Aadnøy & Looyeh, 2011)	- 26 -
Figure (4.5) LAS file for well Moga 7-5	- 28 -
Figure (4.6) showing Poisson Ratio, Shear and young's Modulus Calculations-	29 -
Figure (4.7) overburden pressure VS depth	- 30 -
Figure (4.8) the average pore pressure from sonic and resistivity logs	- 31 -
Figure (4.9) pore pressure and overburden pressure versus depth	- 32 -
Figure (4.10) pore pressure and fracture gradient versus depth	- 33 -
Figure (4.11) Loss circulation occurs in the well	- 35 -
Figure (4.12) The main screen of program	- 36 -

Figure (4.13) result of matlab	- 37 -
Figure (4.14) result of matlab	- 38 -
Figure (4.15) result of matlab	- 39 -
Figure (4.16) result of matlab with entered depth	- 40 -

List of tables

(Table 1.1) :Example of Unplanned Events.(Mitchell, Miska et al. 2011) - 4 -

Chapter 1

Introduction

1.1. Introduction

Wellbore stability is primarily a function of how rocks respond to the induced stress concentration about the wellbore during several drilling activities, such as drillstring movement. In such cases, wellbore stability is impacted by the surge/swab pressure variations from such movement.

Wellbore stability is a very complex phenomenon. Many factors can affect the stress distribution around a borehole during various drilling processes. The main factors that impact wellbore stability-rock properties, far-field principal stresses, wellbore trajectory, pore pressure, drilling fluid and pore fluid chemical properties, temperature, wellbore equivalent mud weight, and time.

Rock properties play a vital role in wellbore stability analysis because the wellbore stability occurs on the rock matrix. Rock types, Young's modulus, Poisson's ratio, Biot's constant, rock porosity, permeability, bulk density, cohesive strength, tensile strength and internal friction angle, natural fractures, etc. are parameters that affect wellbore stability performance .Even though rock properties cannot be controlled by drilling engineers, a better understanding of rock properties can help well planners decrease risk by choosing a different well path or predicting correctly the rock behavior for borehole stability analysis.(F. Zhang et al., 2016)

There are Several well problems often arise during drilling related to the geomechanics and rock behavior and properties such as circulation loss and this is unplanned event that usually must be fixed before drilling can go on. Circulation losses where tensile failure occurred also may lead

to loss of well control, consequential in a blowout, or lead to trouble in cleaning the borehole. Spalling and /or hole closure in case of compressive failure of the rock. Another problem is the Mechanical borehole collapse often happens at low borehole pressures, particularly in shales, chemical effects may induce hole enlargement or collapse. When water-based drilling fluids are used, the shale may react with the mud filtrate (fluid that penetrates the wellbore wall), deteriorating the borehole, hole enlargement, unintentionally induced tensile fractures or difficult directional control incidents. In severe conditions, wellbore instability can increase non-productive time and create simultaneous frequencies of multiple instability incidents, which potentially can lead to stuck pipe, pack off, and eventual loss of the open hole section.(Mondal, Gunasekaran, & K Patel, 2013)

The depleted reservoirs in many oilfields are challenging because of different geomechanical problems arising from wellbore instabilities and overpressure. Therefore, the understanding of geomechanical well construction will minimize the risk of wellbore instability problems, which can dramatically reduce time and cost of field development. To do so, a Mechanical Earth Model (MEM) has been built in this study. A MEM consists of two major parts: rock strength parameters, in-situ stresses and pore pressure.

In (Fig. 1.1) exemplifies some common drilling problems. The mud weight or the bottom hole pressures are often a compromise between well control and borehole stability.

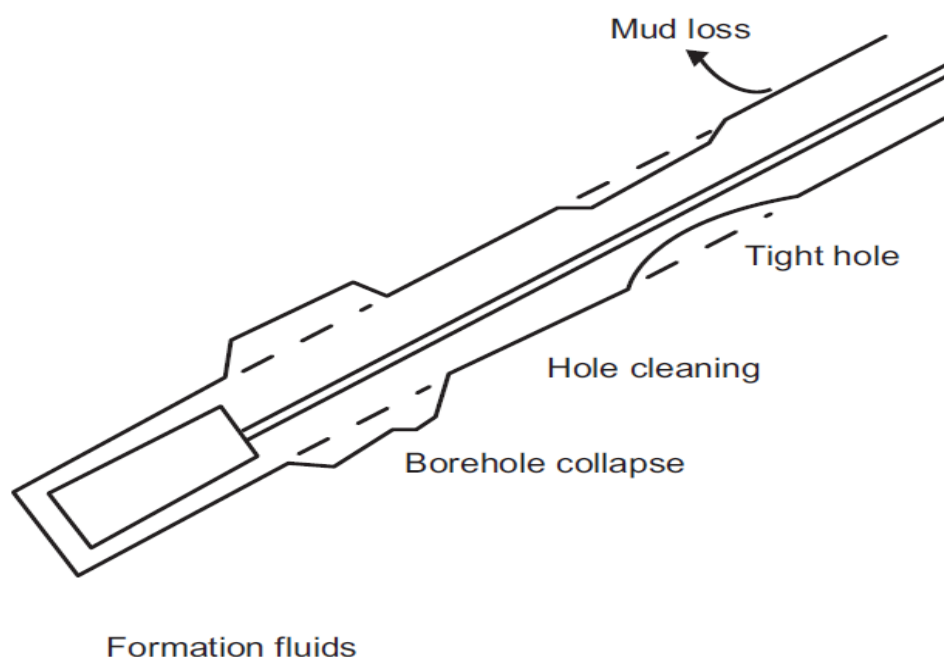


(Fig. 1.1) Typical borehole problems.(Mitchell, Miska, Aadnøy, & Engineers, 2011)

Cost effective and successful drilling requires that the drilling fluid pressure be maintained within a tight mud-weight window dictated by the stress and pressure analyses around the wellbore. The gradient of temperature between the drilling mud and the rock formation is also an important issue in wellbore stability analyses. The temperature gradient will significantly affect the time-dependent stresses and pore pressure distributions around the wellbore. In addition, mud salinity and formation exposure time need to be considered while drilling in chemically reactive formations such as shale, using a water-based mud (WBM).

It is observed that (0.1–0.2days) of consumed time on a well is due to unexpected events. These events often associated with borehole stability. Knowing that the international drilling budgets are many billion dollars, that is mean borehole instability is a huge costly problem. (**Table 1.1**) shows the unexpected time spent the unplanned events in the Table are mostly related to borehole stability. Some wells have lower downtime, but if severe problems arise, they are often very time-consuming to solve.

(Table 1.1) :Example of Unplanned Events.(Mitchell et al., 2011)

Unplanned Event	Time Used to repair
Tight hole, reaming	0.3 days
Squeeze cementing	2.5 days
Mud losses	2.5 days
Fishing	0.3 days
Total time loss	5.6 days
Percent of well	5.6 days / 30 days = 19%

That is prove wellbore instability is so critical and sensitive issue and sequences of it cost a lot of money.

1.2. Objectives:

The objective of this project is to control the stability of wellbore can cause a large fraction of the non-productive time so reducing the number of instability events would lead to less non-productive time and therefore higher cost saving. Since most of these instability events stem from geomechanical reasons, analyzing the geomechanical condition can help increase knowledge about when and where instability could occur

and how it can be prevented. One of the tools of analysis is the mechanical earth model which is subject of this thesis. The main goal of this thesis is to prove that one dimensional mechanical earth model can be used to build reliable safe mud window. In order for this thesis to be able to achieve the mentioned goal.

1.3. Problem statement:

Wellbore instability demonstrates itself in different means like hole pack off, excessive reaming, overpull, torque and drag, sometimes leading to stuck pipe that may require plugging and side tracking. This requires additional time to drill a hole, driving up the cost of drilling operation significantly.

Consequently, in our research we use the rock mechanics and other parameters like pore pressure to find the safe mud weight window which presents the optimum mud weight to be used to prevent the previous problems.

Chapter 2

Literature review

M.R. Mclean and M.A Addis et al (1990) discussed the effect of strength criteria on mud weight recommendations. They proposed a Homogenous, Isotropic, Linear Elastic wellbore stability analysis for the prediction of the onset of failure and consequently the mud weights required to prevent hole instability.(**McLean & Addis, 1990**)

Santarelli et al. (1992) presented a case study of drilling in highly fractured volcanic rocks at great depths. Use of OBM did not solve the problem since the instability was not due to clay. It was found that the main mechanism of instability was mud penetration in fractures which led to eventual erosion of the wellbore wall due to insufficient wall support. Suitable mud weight was designed by simulating the fractured rock mass using discrete element modeling. Use of the new mud weight lower than that being used, along with proper fracture plugging material in WBM proved Successful. Classical method of solving the instability by increasing mud weight could have aggravated the problem.(**Santarelli, Dahen, Baroudi, & Sliman, 1992**)

Al-Buraik and Pasnak (1993) discussed well plans, drilling fluids, casing and cementing liners, logging, completions, and drilling problems encountered in more than a dozen horizontal wells drilled both in sandstone and carbonate reservoirs in Saudi Arabia.(**Al-Buraik & Pasnak, 1993**)

Ezzat (1993) discussed different laboratory tests performed for suitable mud design for drilling Khafji and other reservoirs in Saudi Arabia. Analysis of formation layers showed that the elements of shale causes the well caving, So Use of oil-based mud resulted in reduction of wellbore instability cases. Several studies for mechanical instability have

been conducted to design safe mud weight window using field drilling data. **(Ezzat, 1993)**

Wong et al (Morita and Whitebay, 1994) discussed the Design of wells using principles of rock mechanics in Vineland sand in the Dutch sector of North Sea is reported by Fuh et al. (1991). Using the rock mechanics constraints. A suite of logs was used to predict rock strength, petrophysical properties, and safe mud weight windows (Hassan et al., 1999). Wellbore instability problems were presented in developed field in Italy. The problems were analyzed with respect to the mud type, mud weights, azimuths, and stress regime. The non-inhibitive water-based mud gave better results compared to other mud system **(Santarelli et al, 1996)**.

Santarelli et al. (1996) presented wellbore instability problems occurring in a developed field in Italy. The problems were back analyzed in regard to the mud types, mud weights, azimuths, and stress regime. More drilling problems like reaming and stuck pipe happened in a particular azimuth. This evidenced the existence of anisotropic distribution of horizontal stresses, which was not known because of absence of any in-situ stress related data. **(Santarelli, Zaho, Burrafato, Zausa, & Giacca, 1996)**

Saidin and Smith (2000) discussed wellbore instability encountered when drilling through the Terengganu shale (K-shale), Bekok field, Malaysia. Using (OBM) resulted in formation damage and analysis showed that K-shales had mainly non-reactive weak clay. That helped in improving the design of mud weight window leading to successful completion of a new well. **(Saidin & Smith, 2000)**

Rama Rao, S. Grandi, M.N. Toksov et al (2003) presented geomechanical modeling of in-situ stresses around a borehole. Authors present a modelling of the in-situ stress state associated with the severe

hole enlargement of a wellbore. Geomechanical information is relevant to assure wellbore stability, i.e., to prevent damages in the formation and later on, the casing.(Grandi, 2002).

Zhang, J., W. Standifird and G. Keaney (2006) presented wellbore stability with consideration of pore pressure and drilling fluid interactions. A Poroelastic wellbore stability model incorporating pore pressure and its variation with time is proposed. A finite element method has been developed to couple solid deformation and fluid flow around the wellbore.(J. Zhang, Standifird, & Keaney, 2006)

M.A Moinuddin and K. Khan et al (2006) presented a wellbore stability analysis of vertical, directional and horizontal well using field data. They redeveloped an old offshore field produced using vertical and directional wells by drilling horizontal wells. Quantification of drilling problems in sixty wells show that majority are tight holes along with stuck pipes and hole pack offs problems. The major loss of productivity is due to stuck pipes.(Mohiuddin, Khan, Abdulraheem, Al-Majed, & Awal, 2007)

Jenny Jimenez, Luz Valera Lara, Alexander Rueda and Nestor Fernando Trujillo (2007) discussed the geomechanical wellbore stability modeling of exploratory wells.

Mr. Shams Elfalah Ahmed Alblola from Sudan university (2009) studied greater Bamboo area block 2A of unity in southern Sudan, the study starts by collecting data, evaluating and analyzing, logical arrangement of daily information and the other running operations, run a correlation analyzing, designing, targeting and vise versa to get the optimum. The failure envelope stress, mud pressure and mud weight calculation were done to prevent hole collapse in Bamboo west field.

Chapter 3

Methodology

3.1. Introduction

Through constructing the mechanical earth model (MEM) we can obtain optimum mud weight window. A MEM consists of two major parts: rock strength parameters, in-situ stresses and pore pressure. A properly constructed MEM model flowchart can be depicted as shown in figure 1.

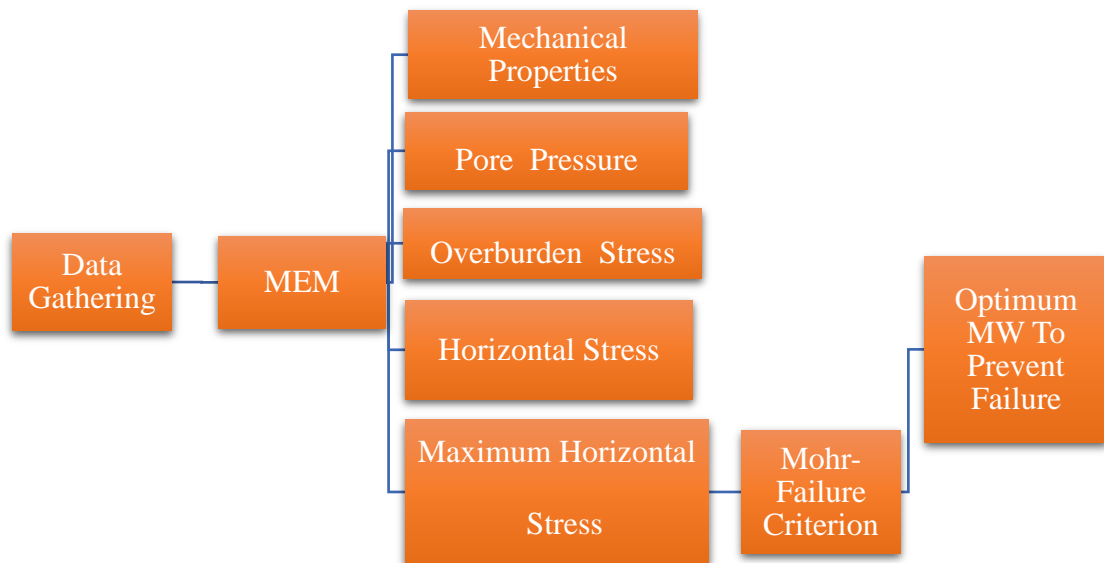


Figure (3.1) Depicted MEM Flowchart

utilizing some software tools (Microsoft Excel and Matlab software program). Before explain design and analysis process it is necessary to briefly explain the Microsoft Excel and Matlab program (GUI).

3.2. Matlab Program (GUI)

The name matlab stands for MATrix LABoratory. matlab was written originally to provide easy access to matrix software developed by the LINPACK (linear system package) and EISPACK (Eigen system package) projects.

Matlab is a high-performance language for technical computing. It integrates computation, visualization, and programming environment. Furthermore, Matlab is a modern programming language environment: it has sophisticated data structures, contains built-in editing and debugging tools, and supports object-oriented programming. These factors make Matlab an excellent tool for teaching and research.

A graphical user interface (GUI) is a graphical display that contains devices, or components, that enable a user to perform interactive tasks. To perform these tasks, the user of the GUI does not have to create a script or type commands at the command line. Often, the user does not have to know the details of the task at hand.

The GUI components can be menus, toolbars, push buttons, radio buttons, list boxes, and sliders-just to name a few. In Matlab, a GUI can also display data in tabular form or as plots, and can group related components.

3.2.1 The GUI contains

- An axes component.
- A pop-up menu listing three data sets that correspond to Matlab functions: peaks, membrane, and sinc.
- A static text component to label the pop-up menu.

- Three buttons that provide different kinds of plots: surface, mesh, and contour When you click a push button, the axes component displays the selected data set using the specified plot.

3.3. Overburden Stress

The overburden stress or vertical stress(σ_v) is induced by the weight of the overlying formations. The typical source to determine it is the density log data. The bulk density is integrated over the overburden depth and multiplied by the gravitational constant to receive the resulting vertical stress. This can be expressed by Eq (1). If a formation is not logged exponential extrapolation is sometimes used to model the unlogged region.(H.Rabia, 2002)

$$\sigma_v = \int \rho(z) g dz \quad \text{Eq. (1)}$$

3.4. Elastic Properties of the Rocks

Young's Modulus (E), shear modulus (G) and Poisson's ratio (v) can be acquired via core analysis and are then called static elastic properties. Doing so only yields information about the depth from which the core was taken. To receive continuous information, the properties are usually derived from sonic log measurements. These are called dynamic elastic properties.

The dynamic elastic properties do not equal the static elastic properties obtained through laboratory tests. This is due to strain magnitude. The acoustic measurements are done using a very small energy pulse which is reversible and so the dynamic moduli are obtained within a perfectly elastic regime. For core measurements, however, large

strains have to be applied during loading, some of which are irreversible. The measured moduli are therefore not purely elastic but introduce additional irreversible deformation caused by friction (plastic part). This means the static strains are always larger than the dynamic strains so the static elastic moduli are always smaller than the dynamic elastic moduli.(Adisornsuapwat, 2013)

The following equations can be used to derive dynamic properties from sonic log data:

$$V_s = 0.7858 - 1.2344 \times V_p + 0.7949 \times V_p^2 - 0.1238 \times V_p^3 + 0.0064 \times V_p^4$$

Eq. (3.2)

Poisson Ratio Calculations :

$$\mu = 0.5 \left(\frac{\left(\frac{\Delta T_s}{\Delta T_c} \right)^2 - 2}{\left(\frac{\Delta T_s}{\Delta T_c} \right)^2 - 1} \right) \quad \text{Eq. (3.3)}$$

Also, we calculate it from Andersons equation:

$$\mu = 0.125q + 0.27 \quad \text{Eq. (3.4)}$$

$$q = \frac{\phi_s - \phi_D}{\phi_s} \quad \text{Eq. (3.5)}$$

Shear Modulus Calculations:

$$G = \rho * 1000 * v_s^2 \quad \text{Eq. (3.6a)}$$

$$G = 1.34 * 10^{10} \frac{A \rho_b}{\Delta T_c^2} \quad \text{Eq. (3.6b)}$$

$$A = \frac{1-2\mu}{2(1-\mu)}$$

Young's Modulus Calculations:

$$E(psi) = 2G(1 + \mu) \quad \text{Eq. (3.7)}$$

In all above equations V_p and V_s represent compression and shear wave velocity (ft/s) respectively. All elastic module used in this research are dynamically calculated. (khair, Zhang, & Abdelrahman, 2015)

3.5. Rock Strength Parameters

The unconfined compressive strength (UCS) and angle of internal friction (ϕ) of sedimentary rocks are key parameters needed to address a range of geomechanical problems ranging from limiting wellbore instabilities during drilling, to assessing sanding potential and quantitatively constraining stress magnitudes using observations of wellbore failure.

Due to the absence of laboratory core measurements, UCS is determined using empirical relationships based on wireline logging measurements. For sandstone reservoirs

$$UCS(MPa) = 258 \exp^{-9\phi} \quad \text{Eq. (3.8)}$$

ϕ = porosity.

The basic equation for calculating porosity from measured logs were as follows: Porosity from density log:

$$\phi_D = \frac{\rho_{ma} - \rho_b}{\rho_{ma} - \rho_b} \quad \text{Eq. (3.9a)}$$

For formation containing shale, the porosity has to be corrected for shale as follows:

$$\phi_D = \frac{\rho_{ma} - \rho_b}{\rho_{ma} - \rho_b} - V_{sh} \left(\frac{\rho_{ma} - \rho_b}{\rho_{ma} - \rho_b} \right) \quad \text{Eq. (3.9b)}$$

Porosity from sonic log the general equation for the porosity calculation from sonic transit time is the relationship proposed by Wyllie (1956)(khair et al., 2015)

$$\phi_s = \left(\frac{\Delta T_{log} - \Delta T_{ma}}{\Delta T_f - \Delta T_{ma}} \right) \quad \text{Eq. (3.10)}$$

3.6. Pore Pressure

Direct measurement of pore pressure in relatively permeable formations is straightforward using a variety of commercially available technologies conveyed either by wireline (samplers that isolate formation pressure from annular pressure in a small area at the wellbore wall) or pipe (packers and drill-stem testing tools that isolate sections intervals of a formation). Similarly, mud weights are sometimes used to estimate pore pressure in permeable formations as they tend to take drilling mud if the mud pressure is significantly in excess of the pore pressure and produce fluids into the well if the converse is true. The pore pressure is an important component in a Mechanical Earth Model and critical to the calculation of horizontal stresses, wellbore stability analysis and other geomechanics applications. Sonic and resistivity logs can be used to identify pore pressure trends which can be used to estimate the pore pressure. The estimated pore pressure needs to be calibrated by pore pressure data.

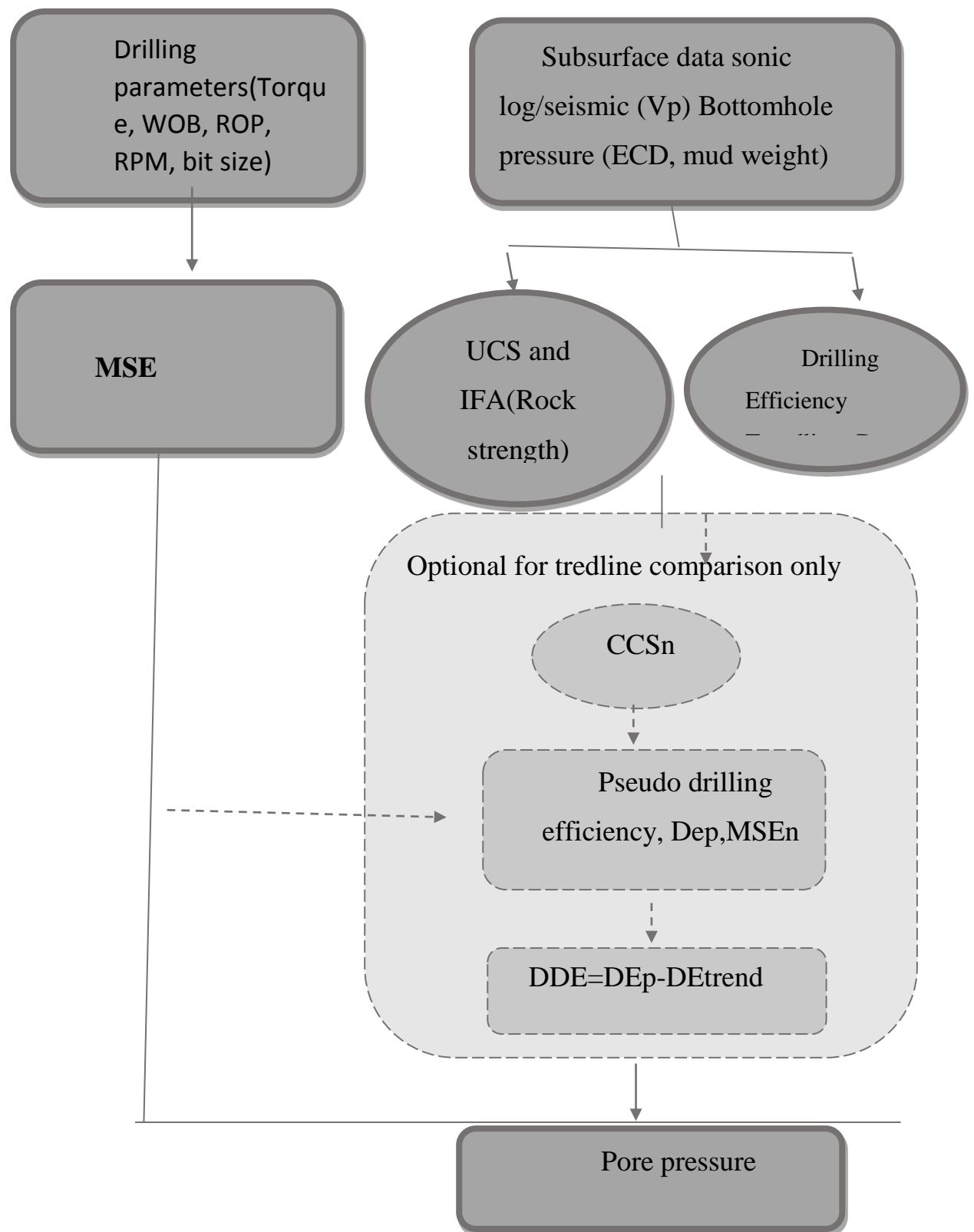


Figure (3.2) Work flow of pore pressure estimation from MSE and DE ('DESME') method.(Zoback, 2007)

3.7.1. Eaton's Method

Eaton's presented the following empirical equation for pore pressure prediction from sonic transient time:

$$Ppg = OBG - (OBG - Png) \left(\frac{\Delta t_n}{\Delta t} \right)^3 \quad \text{Eq. (3.11)}$$

Where Δt_n is the sonic transient time or slowness in shales at the normal pressure; Δt is the sonic transient time in shales obtained from well logging and it can also be derived from seismic interval velocity.

3.7.2.Bowers' Method

Bowers (1995) calculated the effective stresses from measured pore pressure data and overburden stresses and analysed the corresponded sonic velocities from well logging data slope (Zhang 2013). He proposed that the sonic velocity and effective stress have a power relationship as follows:

$$v_p = v_{ml} + A\sigma_e^B \quad \text{Eq(3.12)}$$

Where v_p is the compressional wave velocity at a given depth, v_{ml} is the compressional wave velocity at the mudline, σ_e is the vertical effective stress, A and B are constants for calibration. Using the relationship $\sigma_e = \sigma_v - Pp$ the pore pressure is obtained as:

$$Pp = \sigma_v - \left(\frac{v_p - v_{ml}}{A} \right)^{\frac{1}{B}} \quad \text{Eq. (3.13)}$$

3.7. Minimum Horizontal Stress

There are many available techniques for measuring in situ stress at depth in a wellbore, but all of the methods suffer disadvantages. Core-based methods, including an elastic strain recovery, differential strain curve analysis, shear acoustic anisotropy, acoustic emissions and others, all require the taking of core and detailed analysis. Furthermore, problems with core quality, rock fabric, and other factors may degrade the accuracy of the stress estimate. Direct measurements using small volume hydraulic fractures have fewer analysis problems, but they are expensive and may not be compatible with the well completion scheme, particularly if measurements will be made in layers above the pay zone. The ideal situation would be to measure stress directly from logs, core or drilling data. Attempts to use sonic logs have in some cases given poor results, primarily because of the questionable assumption of elastic uniaxial strain behavior and an uncertain pore-elastic parameter. However, we will be using the normalized Mohr failure envelope approach for different lithologies. The Mohr failure envelope can be obtained from the following normalized equation fit to different lithologies:(McLean & Addis, 1990)

$$\sigma_h = k_o(\sigma_{ob} - P_p) + P_p \quad \text{Eq. (3.14)}$$

Where:

k_o =coefficient for earth at rest, dimensionless.

σ_h = minimum principal in situ stress, psi.

σ_{ob} = overburden stress, psi.

P_p = pore pressure, psi.

k_o in equation (6) is given by

$$Ko = (v/1 - v) \quad \text{Eq. (3.14)}$$

Where

v =Poisson's ratio

3.8. Maximum horizontal stress

Despite the importance of the determination of SH_{max} in geomechanics, it has long been recognized that this is the most difficult component of the stress tensor to accurately estimate, particularly as it cannot be measured directly. Because making stress measurements at great depth offers a unique set of challenges.

Maximum horizontal stress from in situ stress configuration: It is commonly accepted that in situ stress of subsurface formations includes three mutually orthogonal vertical stress, maximum horizontal stress, and minimum horizontal stress. The three principal stresses should satisfy to Hooke's law in order to keep the stress-strain equilibrium. According to Hooke's Law, the minimum horizontal strain can be written as the following formula, when the stresses are expressed in effective stress forms:

$$\varepsilon_h = \frac{\sigma'_h - v(\sigma'_v + \sigma'_H)}{E} \quad \text{Eq. (3.15)}$$

Where ε_h is the strain in the minimum horizontal stress direction; E is the Young's modulus; σ'_v , σ'_H and σ'_h vertical, maximum horizontal and minimum horizontal stresses, respectively. v is the Poisson's ratio

Solve Eq. (3.15)

we have:

$$\sigma'_H = \frac{\sigma'_h - E\varepsilon_h}{v} - \sigma'_v \quad \text{Eq. (3.16)}$$

Normally the formations extend very long in horizontal directions, therefore, the strain in the minimum horizontal direction is much smaller than the strains in vertical and maximum horizontal stress directions. particularly, when the formations of interest are constrained by stiffer formations, the stress state is similar as the condition of uniaxial strain loading is close to zero. Therefore, the upper bound maximum horizontal stress can be expressed as:

$$\sigma'_H \leq \frac{\sigma'_h}{\nu} - \sigma'_v$$

In porous media, the effective stress and total stress have the following relationship:

$$\sigma' = \sigma - \alpha_B Pp \quad \text{Eq. (3.17)}$$

where α_B is the Biot's coefficient. Pp is the pore pressure in the formations. Combine above equations, we have the maximum horizontal stress as follows:

$$\sigma_H \leq \frac{(\sigma_h - \alpha_B Pp)}{\nu} - \sigma_v + 2\alpha_B Pp \quad \text{Eq. (3.18)}$$

We can obtain the upper bound maximum horizontal stress as follows:

$$\sigma_H = \frac{(\sigma_h - Pp)}{\nu} - \sigma_v + 2Pp \quad \text{Eq. (3.19)}$$

maximum horizontal stress can be estimated when we know the minimum horizontal stress, vertical stress, pore pressure and poisson's ratio.

(Spe139280 Maximum Horizontal Stress)

3.9. Internal Friction Angle

It can be determined by correlating physical laboratory test data to a typical downhole log (commonly acoustic or density) by empirical equations

$$\Phi = 26.5 - 37.4(1 - NPHI - Vshale) + 62.1(1 - NPHI - Vshale)^2$$

Eq. (3.20)

Where NPHI is the neutron porosity, and V-shale is the volume of shale obtained by

$$v_{shale} = \frac{GR - GR_{min}}{GR_{max} - GR_{min}} \quad \text{Eq. (3.21)}$$

3.10. Fracture gradient

The Hubbert and Willis method is based on the principle that fracturing occurs when the applied fluid pressure exceeds the sum of the minimum effective stress and formation pressure. The fracture plane is assumed to be always perpendicular to the minimum principal stress. According to the Hubbert and Willis method, the total injection (or fracturing) pressure required to keep open and extend a fracture is given by:

$$FG = \sigma'_3 + Pf \quad \text{Eq. (3.22)}$$

where σ'_3 is the effective minimum principal stress.

In terms of overburden gradient, Poisson's ratio (ν) and formation pressure, the above equation becomes:(H.Rabia, 2002)

$$FG = \left(\frac{\nu}{1-\nu} \right) \left(\frac{(\sigma_v - Pf)}{D} \right) + \frac{pf}{D} \quad \text{Eq. (3.22)}$$

3.11. Mohr-coulomb failure criterion

This criterion relates the shearing resistance to the contact forces and friction, to the physical bonds that exist among the rock grains. For practical rock failure analyses, it could be useful to find expressions for the particular stress state. The failure point (σ, τ) is expressed as:

$$\tau = \frac{1}{2}(\sigma_1 - \sigma_3)\cos\phi \quad \text{Eq. (3.23)}$$

$$\sigma = \frac{1}{2}(\sigma_1 + \sigma_3) - \frac{1}{2}(\sigma_1 - \sigma_3)\sin\phi \quad \text{Eq. (3.24)}$$

Where: τ is the shear stress, ϕ is the angle of internal friction.(Aadnøy & Looyeh, 2011)

3.12. Estimating Tensile strength

There is a strong correlation between the tensile strength and the unconfined compressive strength. It is possible, but not recommended, to fit only the triaxial and UCS data, and then estimate the tensile strength by calculating m_i (Hoek and Brown 1997). Where m_i is a material constant for the intact rock which depends only upon the rock type (texture and mineralogy). We notice that it is 17 ± 4 for sandstone rocks. If only UCS testing has been completed and reliable tensile testing data are unavailable an estimate can be made using:

$$\sigma_t = -\frac{UCS}{m_i} \quad \text{Eq. (3.25)}$$

Chapter 4

Results and Discussion

4.1. The quantification of wellbore instability:

The quantification of wellbore instability requires the understanding and quantifying of

steps:

1. Determining magnitude and direction of in-situ earth stresses.
2. Determining rock properties.
3. Establishing a rock failure criterion.
4. Calculation of induced stresses around the wellbore for well
5. Compare the induced stresses with the stresses from failure criterion to establish

If the wellbore will fail.

4.1.1. Determining magnitude and direction of in-situ earth stresses

There are three ways to determine earth stresses:

4.1.1.1. Fracture tests

Formation is fractured by using a drilling mud density that is greater than the formation breakdown pressure to stimulate hydrocarbon production by increasing the formation permeability. Laboratory tests have shown that fractures formed by hydraulic fracturing operations propagate perpendicular to the minor principal stress.

Following the initiation and extension of a fracture, the borehole fluid pressure is reduced to allow the fracture to close. The pressure is then gradually increased by pumping fluid into the borehole and the relationship between the volume pumped and the pressure increase is monitored. When the relationship becomes non-linear the fracture is

assumed to have reopened; the pressure at this point is equal to, and counteracts, the stress perpendicular to the fracture face, shown experimentally to be the minor principal stress. fractures when the circumferential stress at the borehole wall equals the rock the strength. The stress is actually an induced stress as a result of drilling the.

4.1.1.2. Open- hole Caliper Surveys

The caliper tool has 2,30r 4 arms and its used to measure the radius of the well. If the orientation of the tool is referenced to grid north, therefore the azimuth of the minimum principal stress is

4.1.1.3. The Application of Linear Elastic Theory

It's applied when no fracture and logging data are available to determine the magnitude and direction of the in-situ stress field, linear elastic theory can be applied to calculate the principal stresses. Its assumptions:

- An isotropic, homogeneous rock mass.
- The principal stresses are orientated vertically and horizontally.
- No tectonic forces are acting, and therefore the horizontal principal stresses are equal.
- The vertical principal stress equals the overburden stress.
- The rock material is linear elastic.

4.1.2. Determination of rock properties:

Passion's Ratio

$$\mu = 0.5 \left(\frac{\left(\frac{\Delta T_S}{\Delta T_C} \right)^2 - 2}{\left(\frac{\Delta T_S}{\Delta T_C} \right)^2 - 1} \right)$$

Shear Modulus Calculations:

$$G = \rho * 1000 * v_s^2$$

Young's Modulus Calculations:

$$E(\text{psi}) = 2G(1 + \mu)$$

4.1.3. Rock failure:

If cores are tested in a triaxial testing machine where axial stress (σ_1) is applied in one direction and a confining stress (σ_3), then by varying the magnitude of the Confining pressure the rock will fail in shear at different values of σ_1 .

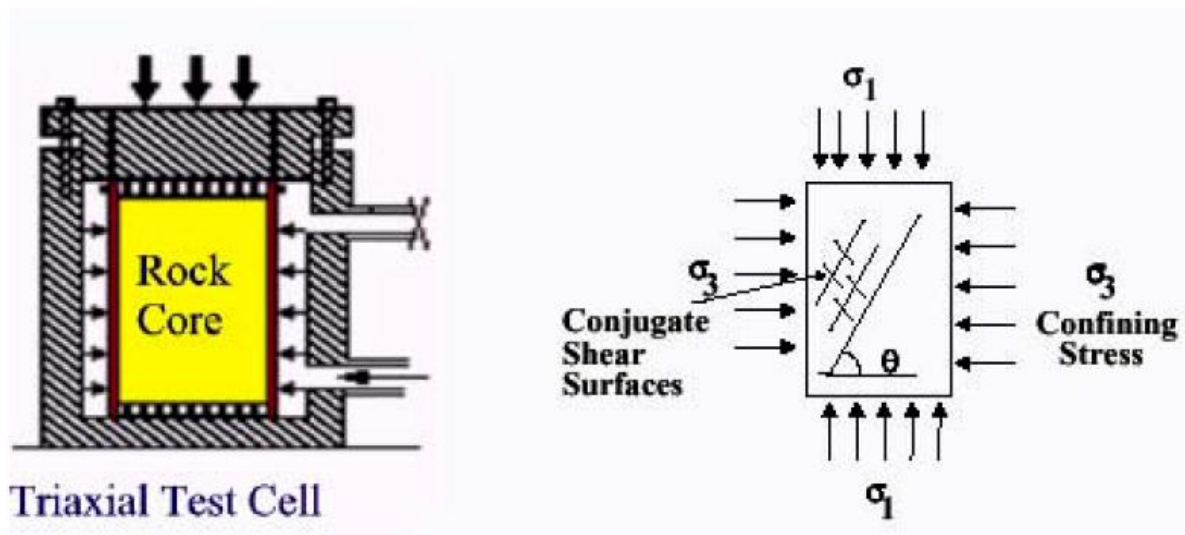


Figure (4-1) Triaxial Rock Testing.(H.Rabia, 2002)

In Mohr plot shear stress is plotted against principal stress. The principal stresses (σ_1 and σ_3) are plotted on the horizontal axis and shear stresses are on the vertical. A circle is then drawn

through these values with a diameter equal to $(\sigma_1 - \sigma_3)$ and center equal to $1/2 (\sigma_1 + \sigma_3)$. A tangent (which can be linear or curve) is drawn to this circle which represents the failure envelope. Below this envelope the rock is stable. Above its rock failure occurs.

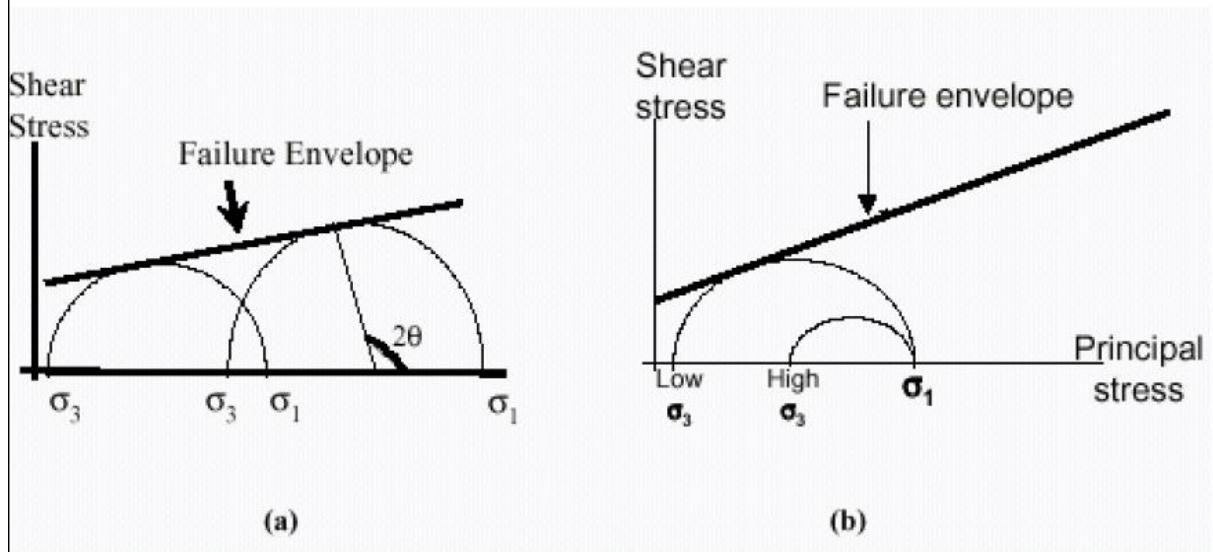


Figure (4-2) Mohr Envelop. (H.Rabia, 2002)

4.1.3.1 Mohr-Coulomb Criterion:

the failure criterion states the shear stress across a plane is resisted by the cohesion and normal stress such that:

$$|t| = C + \sigma \tan \phi$$

Mohr circles represent the basis of this failure criterion. For practical rock failure analyses, it could be useful to find expressions for the particular stress state. Assuming the stresses of Figure (4.2) represent the effective stresses, the failure point (σ, τ) is expressed as:

$$\tau = \frac{1}{2}(\sigma_1 - \sigma_3)\cos\phi$$

$$\sigma = \frac{1}{2}(\sigma_1 + \sigma_3) - \frac{1}{2}(\sigma_1 - \sigma_3)\sin\phi$$

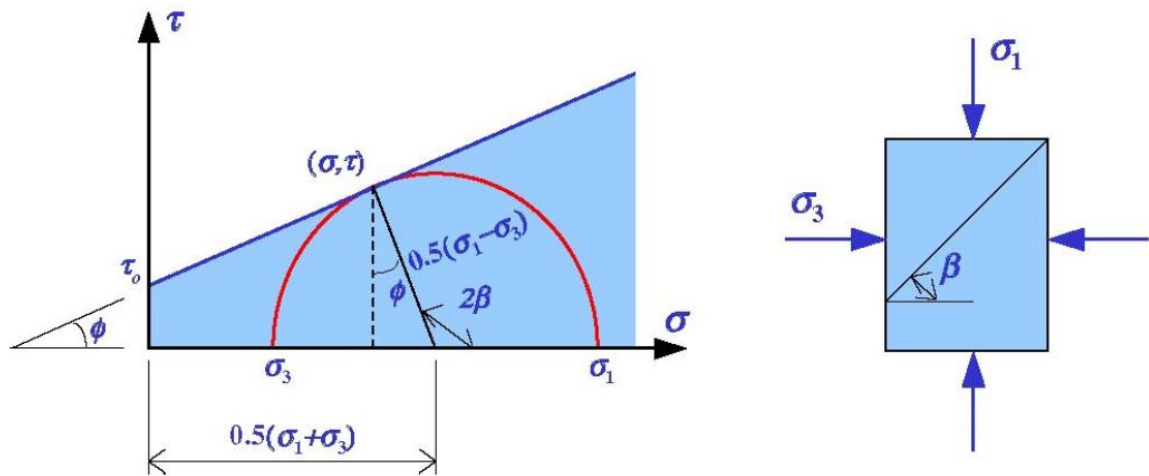


Figure (4-3) Failure stresses using the triaxial test results and Mohr-Coulomb model.(Aadnøy & Looyeh, 2011)

The drawbacks of the Mohr-Coulomb criterion:

1-The criterion does not consider the intermediate principal stress(σ_2).

2-t implies that a major shear fracture occurs at peak strength.

3-It implies a direction of shear, relative to the major and minor principal stresses.

4-Experimental peak strength envelopes derived using the Mohr constructions are generally non-linear.(H.Rabia, 2002)

4.2. Procedures for determining safe mud weights to prevent hole collapse:

- i. Determine the three in-situ stresses σ_1 , σ_2 and σ_3 .
- ii. Determine which failure criterion to use:

The Mohr-Coulomb failure criterion, where:

$$\tau = \frac{1}{2}(\sigma_1 - \sigma_3)\cos\phi$$

$$\sigma = \frac{1}{2}(\sigma_1 + \sigma_3) - \frac{1}{2}(\sigma_1 - \sigma_3)\sin\phi$$

- iii. Determine the cohesion and angle of internal friction from laboratory testing (triaxial testing) Of cores from offset wells.
- iv. Calculate the failure surface from The Mohr-coulomb criterion as follow:

$$(\sigma_1 - Pf) = \frac{1 + \sin\phi}{1 - \sin\phi}(\sigma_3 - pf) + \frac{2\cos\phi}{1 - \sin\phi}$$

4.3. Calculations

The data that have been collected is as LAS file which content of log data as follows

depth	BIT	CAL	CNC	DT	GR	KINT_GEO_QEPP	PE	PIGE_QEPP	RD	RMSL	RS	SPBR	SW_QE	VCL_GEO_ZDEN
480.7459	9.875	10.826	38.997	134.067	88.061	4.542549	2.57	0.2106544	4.304	0.704	2.092	159.668	0.925585	0.346129
480.8221	9.875	10.826	39.829	133.999	89.491	4.79631	2.366	0.2208087	4.433	0.625	2.167	160.274	0.958737	0.347637
480.8983	9.875	10.827	44.764	134.234	90.812	0.7950096	2.378	0.2093298	4.517	0.646	2.22	160.869	0.980527	0.45041
480.9745	9.875	10.828	51.653	134.751	91.603	0.04584991	2.531	0.1815949	4.539	0.758	2.242	161.435	0.989879	0.608831
481.0507	9.875	10.826	56.075	135.434	93	0.005075922	2.63	0.1540677	4.489	0.899	2.225	161.963	0.997723	0.72571
481.1269	9.875	10.819	55.321	136.144	95.229	0.005780174	2.925	0.1518389	4.368	0.967	2.17	162.458	0.961419	0.715362
481.2031	9.875	10.804	52.999	136.802	98.299	0.01200752	3.213	0.1542874	4.189	0.977	2.084	162.93	0.938614	0.67191
481.2793	9.875	10.78	50.338	137.381	102.551	0.03581833	3.528	0.1626062	3.981	0.994	1.981	163.392	0.89687	0.609813
481.3555	9.875	10.749	47.178	137.828	108.641	0.08203899	3.317	0.1615457	3.778	0.975	1.88	163.859	0.899778	0.558649
481.4317	9.875	10.715	43.118	138.027	115.281	0.4268094	2.893	0.1749945	3.616	0.876	1.798	164.344	0.900732	0.46817
481.5079	9.875	10.684	39.839	137.837	118.968	1.902748	2.77	0.1901302	3.52	0.766	1.748	164.857	0.913079	0.388557
481.5841	9.875	10.661	40.377	137.189	117.45	2.144927	2.63	0.1982228	3.502	0.704	1.733	165.41	0.925434	0.386235
481.6603	9.875	10.648	44.251	136.091	111.07	0.606923	2.707	0.1946194	3.556	0.699	1.752	166.007	0.938287	0.459415
481.7365	9.875	10.644	49.113	134.593	103.043	0.08625827	2.755	0.1787204	3.666	0.74	1.797	166.646	0.964227	0.56789
481.8127	9.875	10.643	52.059	132.77	97.476	0.02111312	2.834	0.1625574	3.808	0.808	1.858	167.315	0.983217	0.643629

Figure (4.5) LAS file for well Moga 7-5

4.3.1. Poisson Ratio, Shear and young's Modulus Calculations

$$\mu = 0.5 \left(\frac{\left(\frac{\Delta T_s}{\Delta T_c} \right)^2 - 2}{\left(\frac{\Delta T_s}{\Delta T_c} \right)^2 - 1} \right) \quad (3)$$

We calculate it from Andersons equation:

$$\mu = 0.125q + 0.27$$

$$q = \frac{\phi_s - \phi_D}{\phi_s}$$

Shear Modulus Calculations:

$$G = \rho * 1000 * V_s^2 \quad (4)$$

$$G = 1.34 * 10^{10} \frac{A\rho_b}{\Delta T c^2}$$

$$A = \frac{1 - 2\mu}{2(1 - \mu)}$$

$$B = \frac{1 + \mu}{3(1 - \mu)}$$

Young's Modulus Calculations:

$$E(psi) = 2G(1 + \mu)$$

We get the following

DEPT	DT	ZDEN	Pro (s)	Pro(d)	q	Poisson	A	B	KB	G	E
548.7925	138.721	2.072	0.625343	0.350303	0.439822	0.324978	0.259284	0.654289	944016.1	374097.9	991342.6998
548.8687	139.653	2.055	0.632288	0.360606	0.42968	0.32371	0.260672	0.652437	921201.8	368053.3	974391.704
548.9449	140.379	2.05	0.637697	0.363636	0.429767	0.323721	0.26066	0.652453	909501.7	363353.5	961957.2093
549.0211	140.871	2.044	0.641364	0.367273	0.427356	0.32342	0.26099	0.652014	899910.6	360218.2	953439.6205
549.0973	141.104	2.039	0.6431	0.370303	0.42419	0.323024	0.261422	0.651438	893956.5	358744.1	949254.0971
549.1735	140.963	2.034	0.642049	0.373333	0.418528	0.322316	0.262193	0.650409	892138.5	359638.7	951112.1627
549.2497	140.329	2.032	0.637325	0.374545	0.412316	0.32154	0.263037	0.649283	897776	363706.5	961305.1512
549.3259	139.301	2.037	0.629665	0.371515	0.409979	0.321247	0.263355	0.648861	912722.5	370448.8	978909.0214
549.4021	138.288	2.043	0.622116	0.367879	0.408666	0.321083	0.263533	0.648623	928531.2	377258.3	996779.0941
549.4783	137.755	2.044	0.618145	0.367273	0.405847	0.320731	0.263915	0.648114	935453.3	380920.8	1006187.646
549.5545	137.875	2.039	0.619039	0.370303	0.40181	0.320226	0.264461	0.647385	930494.1	380113.2	1003670.804
549.6307	138.387	2.03	0.622854	0.375758	0.396716	0.31959	0.265149	0.646467	918241.4	376617.9	993962.1021
549.7069	138.873	2.021	0.626475	0.381212	0.391497	0.318937	0.265853	0.645529	906465.2	373316.9	984763.0783
549.7831	139.179	2.019	0.628756	0.382424	0.391776	0.318972	0.265816	0.645579	901660.5	371256.9	979354.7902
549.8593	139.495	2.017	0.631111	0.383636	0.392125	0.319016	0.265769	0.645642	896777.9	369145.4	973816.9779
549.9355	140.03	2.013	0.635097	0.386061	0.392123	0.319015	0.265769	0.645641	888173.3	365603.8	964474.1134
550.0117	140.714	2.018	0.640194	0.38303	0.401696	0.320212	0.264477	0.647365	884097.8	361192.3	953700.8573
550.0879	141.213	2.025	0.643912	0.378788	0.41174	0.321467	0.263116	0.649179	883374.8	358036.4	946266.8545
550.1641	141.198	2.032	0.6438	0.374545	0.418227	0.322278	0.262234	0.650355	888222.4	358146.1	947137.8321
550.2403	140.624	2.035	0.639523	0.372727	0.417179	0.322147	0.262376	0.650165	896548.3	361805.6	956720.5762
550.3165	139.686	2.053	0.632534	0.361818	0.427986	0.323498	0.260904	0.652128	919435.2	367847.8	973691.742
550.3927	138.597	2.062	0.624419	0.356364	0.429287	0.323661	0.260726	0.652366	938375.8	375033.3	992833.9388
550.4689	137.519	2.047	0.616386	0.365455	0.407101	0.320888	0.263745	0.64834	940373.1	382543.8	1010594.704

Figure (4.6) showing Poisson Ratio, Shear and young's Modulus Calculations

the average result is of well is

$$\mu=0.3237$$

$$G=8.37E5 \text{ PSI}$$

$$E= 2.2E6 \text{ PSI}$$

4.3.2.Overburden pressure:

$$\sigma_v = \int \rho(z) g dz$$

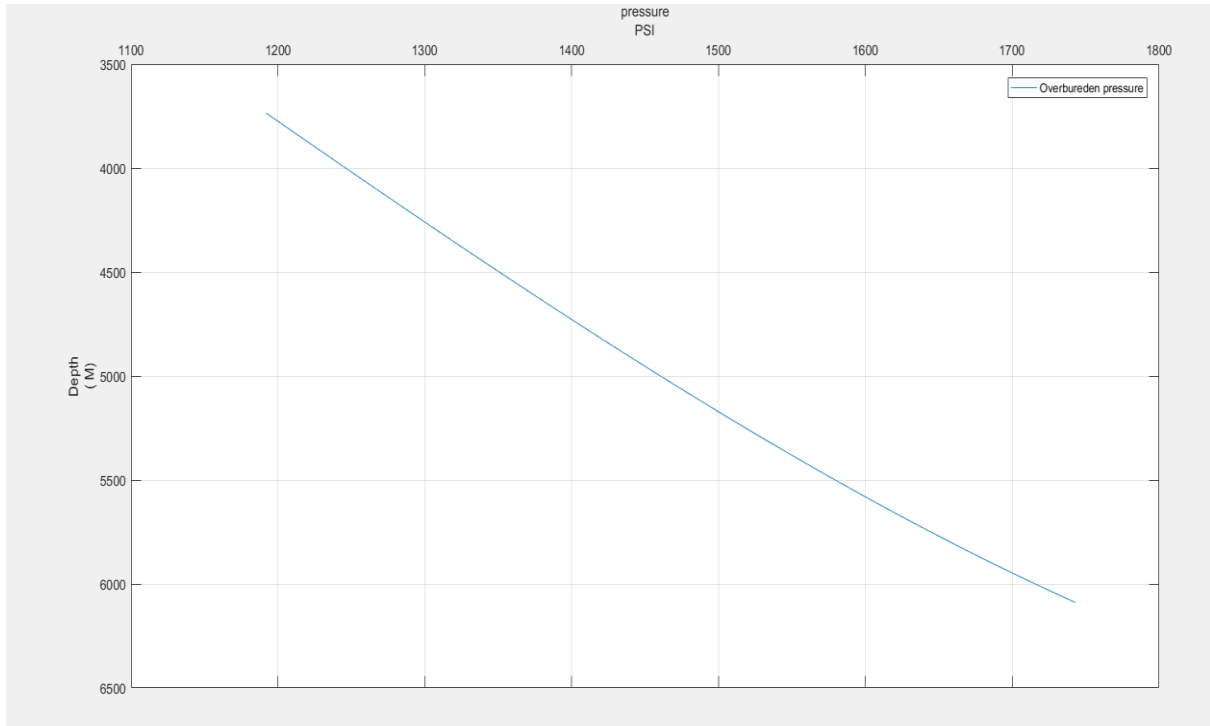


Figure (4.7) overburden pressure VS depth

Pore pressure:

the pore pressure can be calculated from density log and resistivity log with many methods. In our case, we used Eaton's method according to the following equations

$$P_{pg} = OBG - (OBG - P_{ng}) \left(\frac{\Delta t_n}{\Delta t} \right)^3$$

$$P_p = \sigma_v - (\sigma_v - P_n) * \left(\frac{R}{R_n} \right)^n$$

And then by taking the average value after that induces the equation of curve as function of depth by interpolation

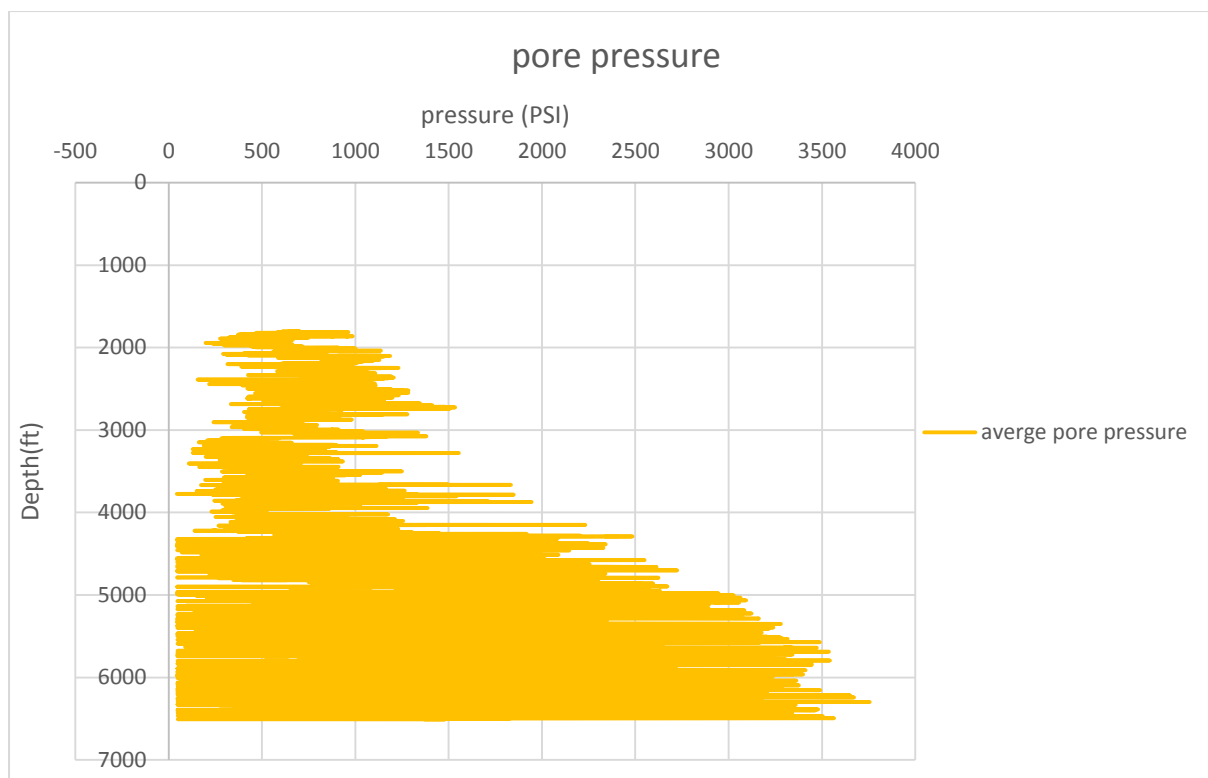


Figure (4.8) the average pore pressure from sonic and resistivity logs

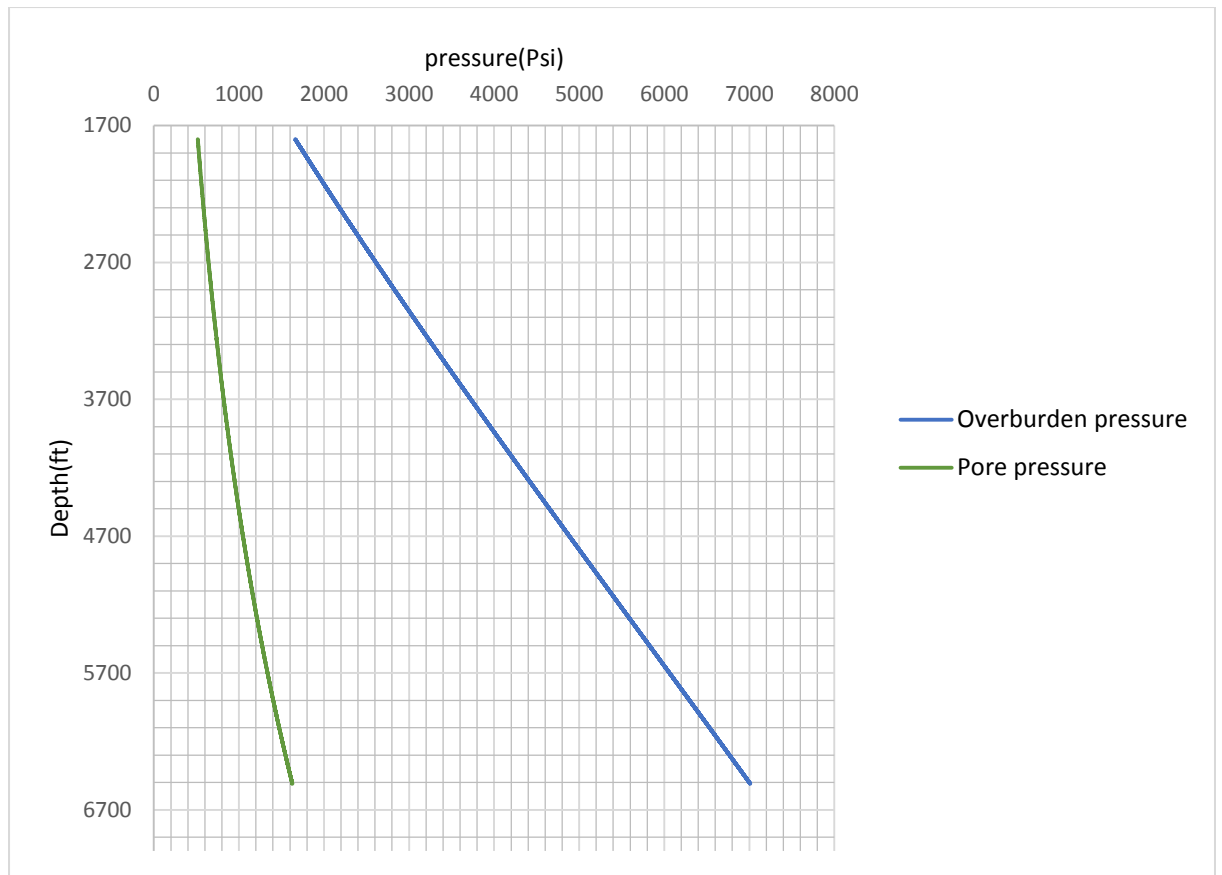


Figure (4.9) pore pressure and overburden pressure versus depth

Minimum horizontal stress:

$$\sigma_h = K_o(\sigma_{ob} - P_p) + P_p$$

$$K_o = \frac{\nu}{1-\nu}$$

Fracture pressure:

$$FG = \sigma'_3 + P_f$$

The range between the fracture pressure and pore pressure consider as mud window for safe drilling without the predicted problems that occur due to increase or decrease the mud weight and its showing below.

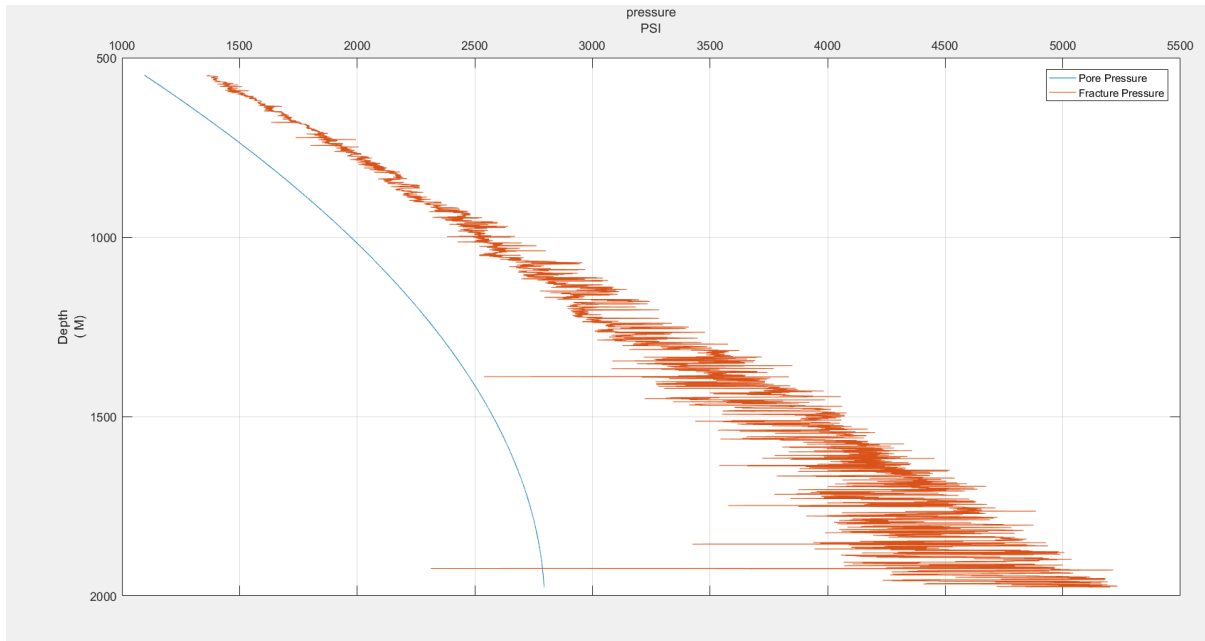


Figure (4.10) pore pressure and fracture gradient versus depth

Optimum mud weight:

According to the chart and equation above we can determine the optimum mud weight based on the following equations:

$$p_{mud} \geq 3\sigma_H - \sigma_h - P_p - UCS$$

$$p_{mud} \leq 3\sigma_h - \sigma_H - p_p + T$$

4.4. Result:

General information about the field:

Fula sub basin

The Fula sub-basin is a fault-bounded depression located in the NE of the Muglad Basin, Sudan, and covers an area of about 3560 km². Eleven oilfields and oil-bearing structures have been discovered in the sub-basin. The Lower Cretaceous Abu Gabra shales (Barremian – Aptian), deposited in a deep-water lacustrine environment, are major source rocks. Reservoir targets include interbedded sandstones within the Abu Gabra Formation and sandstones in the overlying Bentiu and Aradeiba Formations (Albian – Cenomanian and Turonian, respectively). Oil-source correlation indicates that crude oils in the Aradeiba and Bentiu Formations are characterized by low APIs (<22°), low Sulphur contents (<0.2%), high viscosity and high Total Acid Number (TAN: >6 mg KOH/g oil on average). By contrast, API, viscosity and TAN for oils in the Abu Gabra Formation vary widely. These differences indicate that oil migration and accumulation in the Fula sub-basin is more complicated than in other parts of the Muglad Basin, probably as a result of regional transtension and inversion during the Late Cretaceous and Tertiary. The Aradeiba-Bentiu and Abu Gabra Formations form separate exploration targets in the Fula sub-basin. Four play fairways are identified: the central oblique anticline zone, boundary fault zone, fault terrace zone and sag zone. The most prospective locations are probably located in the central oblique anticline zone. (D, Dingsheng, Zhi, Zhiwei, & Jingchun, 2013)

In Moga 7-5 well there is total loss of circulation detected at depth of 1310m to 1320m by loss of 83.9m³ and the report showed the mud weight that used is 11.8ppg which caused the fracture of formation which lead to mud loss.

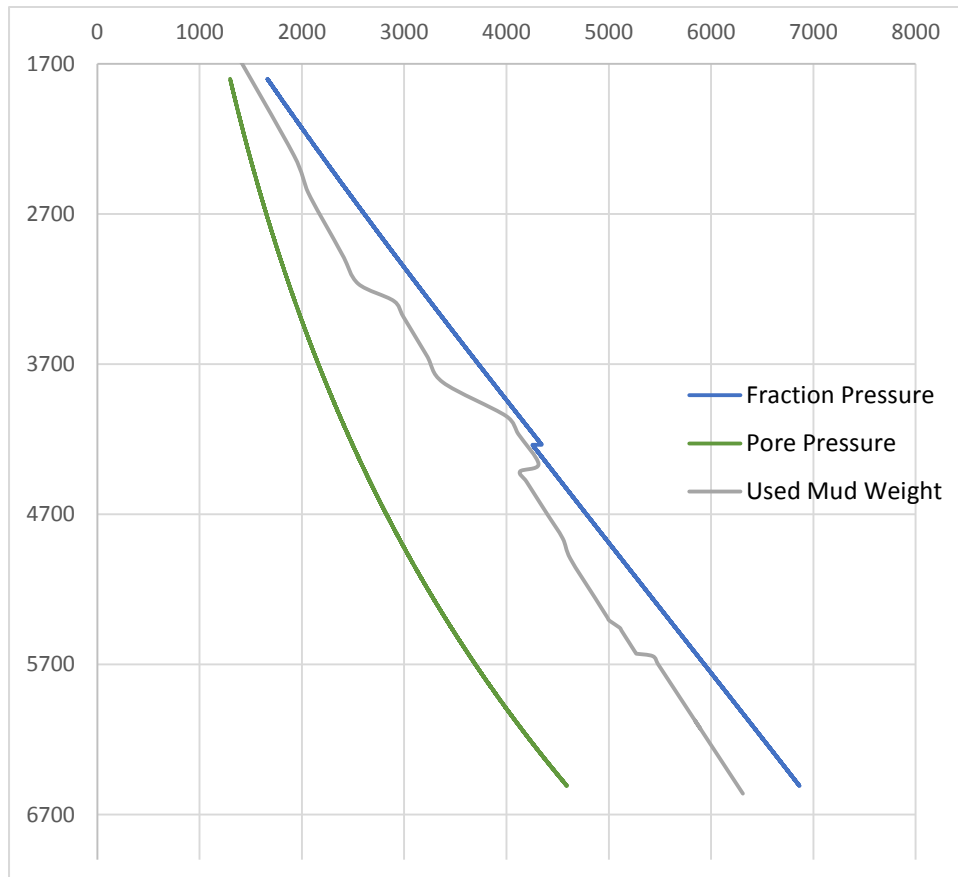


Figure (4.11) Loss circulation occurs in the well

From our study the optimum mud weight is 10.5

Matlab Program:

A program used to calculate the pore pressure, overburden pressure, fraction pressure, minimum horizontal stress, and Mohr failure line and plot of curves.

The input data as excel sheet with type (*.xls, *.xlsx).

Depth (m)	Used mud weight (ppg)	Optimum mud weight (ppg)
1000	10.9	10
1100	11	10.2
1200	11.3	10.5
1300	11.8	10.7
1500	12.3	11

OMW Calculator

Load Data

	Depth ,m	CNC	DT	GR	ZDEI
1					
2					
3					
4					

Show Data as plots

Calculate Data

	Depth ,m
1	
2	
3	
4	
5	
6	

	EMW ,PPG	Pp ,PSI	Fracure Press. ,PSI

Figure (4.12) The main screen of program

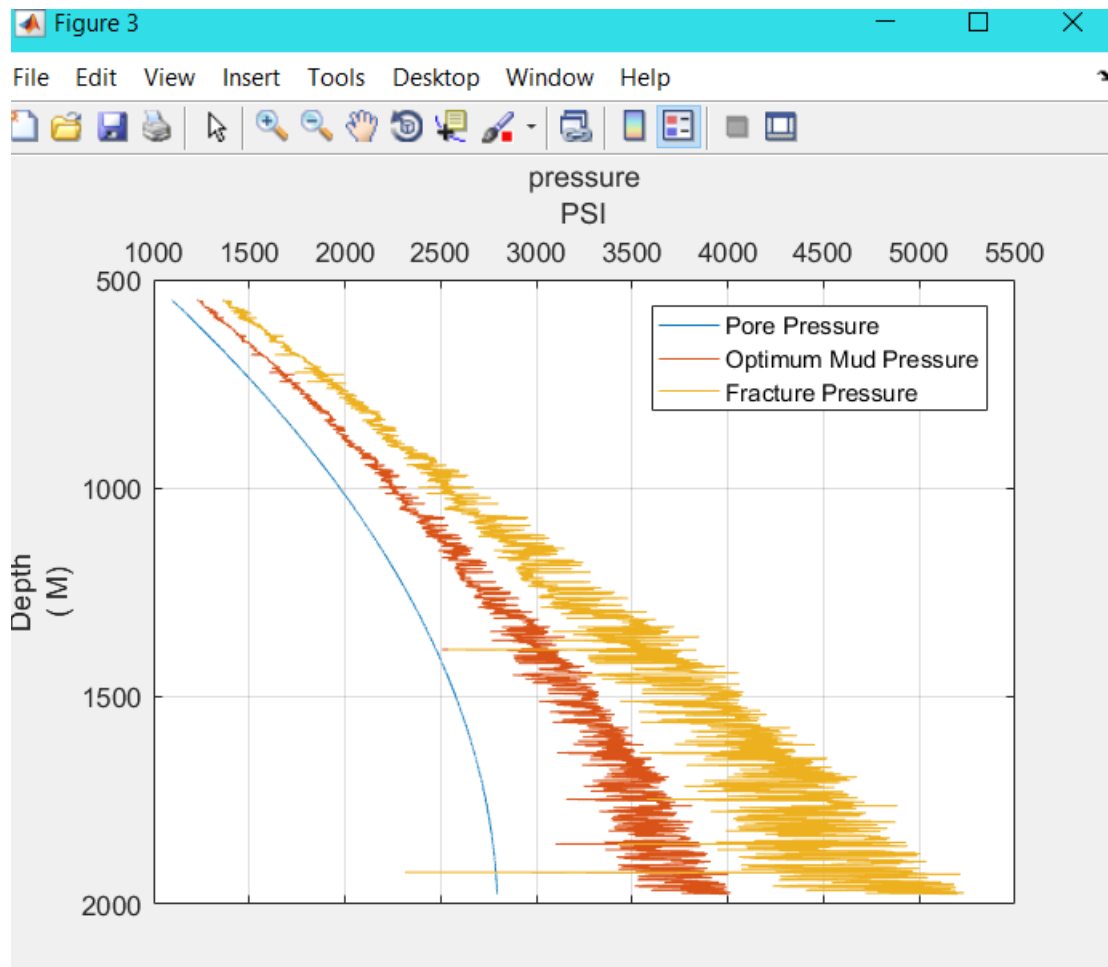


Figure (4.13) result of matlab

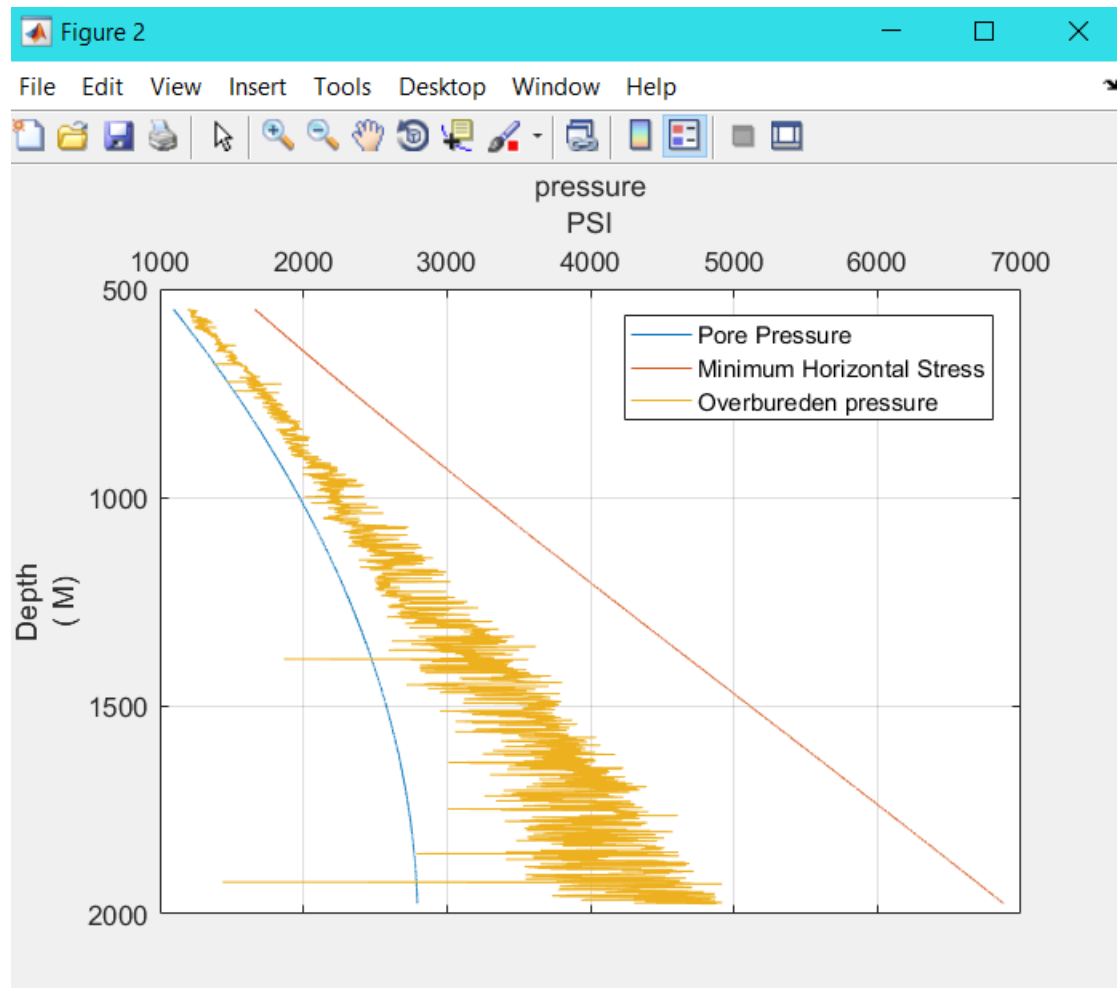


Figure (4.14) result of matlab

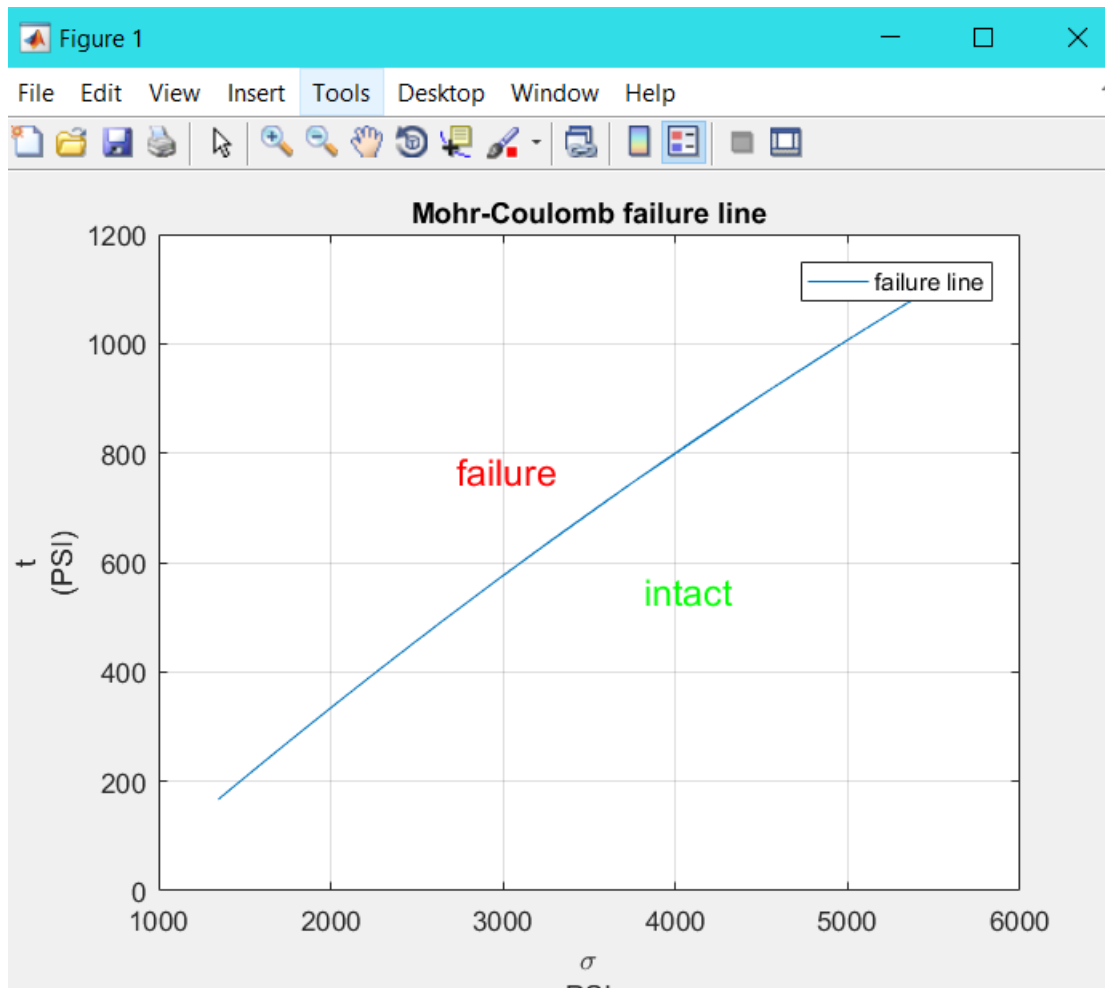


Figure (4.15) result of matlab

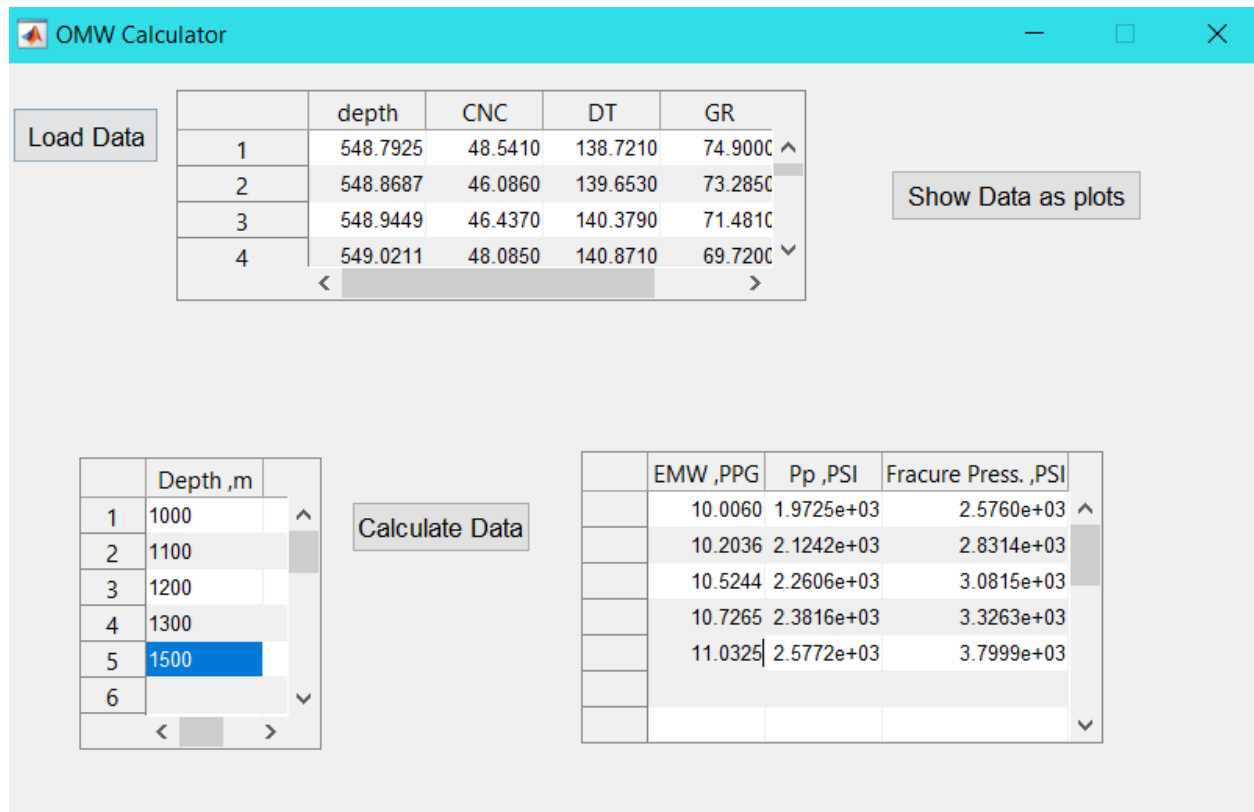


Figure (4.16) result of matlab with entered depth

Chapter 5

Conclusion and Recommendation

Geomechanical modeling is playing an increasingly important role at challenging field development projects since field development decisions are aided by an accurate assessment of well design options that are closely tied to the existing geological and engineering data set using geomechanics modeling.

In this study, it was tried to employ an elastoplastic model to find the mud weight in which a well is stable when having no safe mud weight window.

From MEM, an obvious change in the profiles of pore pressure, shear failure, and fracture gradients are visible for the interval between 1310m up to 1320m. The used mud weight for drilling this section has reached the fracture gradient causing loss circulation. The interval from 1310m down to TD has higher pore pressure, shear failure, and fracture gradients.

It is recommended to perform some laboratory core measurements for rock strength parameters, to calibrate log data It is recommended to use and update this model during drilling of new wells in the field, because real time geomechanics support allowed making important decisions in time when unplanned events occurred while drilling.

References

- Aadnøy, B., & Looyeh, R. (2011). Chapter 5 - Failure Criteria *Petroleum Rock Mechanics* (pp. 53-62). Boston: Gulf Professional Publishing.
- Adisornsuapwat. (2013).
- Al-Buraik, K. A., & Pasnak, J. M. (1993). *Horizontal Drilling in Saudi Arabian Oil Fields: Case Histories*. Paper presented at the Middle East Oil Show, Bahrain.
- D, L., Dingsheng, C., Zhi, L., Zhiwei, Z., & Jingchun, W. (2013). *Petroleum geology of the fula sub-basin, Muglad basin, Sudan* (Vol. 36).
- Ezzat, A. M. (1993). *Horizontal Drilling and Completion Fluids Design Criteria*. Paper presented at the Middle East Oil Show, Bahrain.
- Grandi, S., Rao, R, Toksoz, MN. (2002). Geomechanical modeling of in-situ stresses around a borehole.
- H.Rabia. (2002). well engineering and construction rabia.
- khair, E. M. M., Zhang, S., & Abdelrahman, I. M. (2015). *Correlation of Rock Mechanic Properties with Wireline Log Porosities through Fulla Oilfield - Muglad Basin -Sudan*. Paper presented at the SPE North Africa Technical Conference and Exhibition, Cairo, Egypt. <https://doi.org/10.2118/175823-MS>
- McLean, M. R., & Addis, M. A. (1990). *Wellbore Stability: The Effect of Strength Criteria on Mud Weight Recommendations*. Paper presented at the SPE Annual Technical Conference and Exhibition, New Orleans, Louisiana.
- Mitchell, R. F., Miska, S., Aadnøy, B. S., & Engineers, S. o. P. (2011). *Fundamentals of Drilling Engineering*: Society of Petroleum Engineers.
- Mohiuddin, M. A., Khan, K., Abdurraheem, A., Al-Majed, A., & Awal, M. R. (2007). Analysis of wellbore instability in vertical, directional, and horizontal wells using field data. *Journal of Petroleum Science and Engineering*, 55(1), 83-92. doi: <https://doi.org/10.1016/j.petrol.2006.04.021>
- Mondal, S., Gunasekaran, K., & K Patel, B. (2013). *Predrill wellbore stability analysis using rock physical parameters for a deepwater high angle well: A case study*.
- Saidin, S., & Smith, S. P. T. (2000). *Wellbore Stability And Formation Damage Considerations For Bekok Field K Formation*. Paper presented at the IADC/SPE Asia Pacific Drilling Technology, Kuala Lumpur, Malaysia.
- Santarelli, F. J., Dahren, D., Baroudi, H., & Sliman, K. B. (1992). Mechanisms of borehole instability in heavily fractured rock media. *International Journal of Rock Mechanics and Mining Sciences & Geomechanics Abstracts*, 29(5), 457-467. doi: [https://doi.org/10.1016/0148-9062\(92\)92630-U](https://doi.org/10.1016/0148-9062(92)92630-U)
- Santarelli, F. J., Zaho, S., Burrafato, G., Zausa, F., & Giacca, D. (1996). *Wellbore Stability Analysis Made Easy and Practical*. Paper presented at the SPE/IADC Drilling Conference, New Orleans, Louisiana.
- Zhang, F., Kang, Y., Wang, Z., Miska, S., Yu, M., & Zamanipour, Z. (2016). *Real-Time Wellbore Stability Evaluation for Deepwater Drilling During Tripping*. Paper presented at the SPE Deepwater Drilling and Completions Conference, Galveston, Texas, USA. <https://doi.org/10.2118/180307-MS>
- Zhang, J., Standifird, W., & Keaney, G. (2006). *Wellbore stability with consideration of pore pressure and drilling fluid interactions*.
- Zoback, M. D. (2007). *Reservoir Geomechanics*. Cambridge: Cambridge University Press.